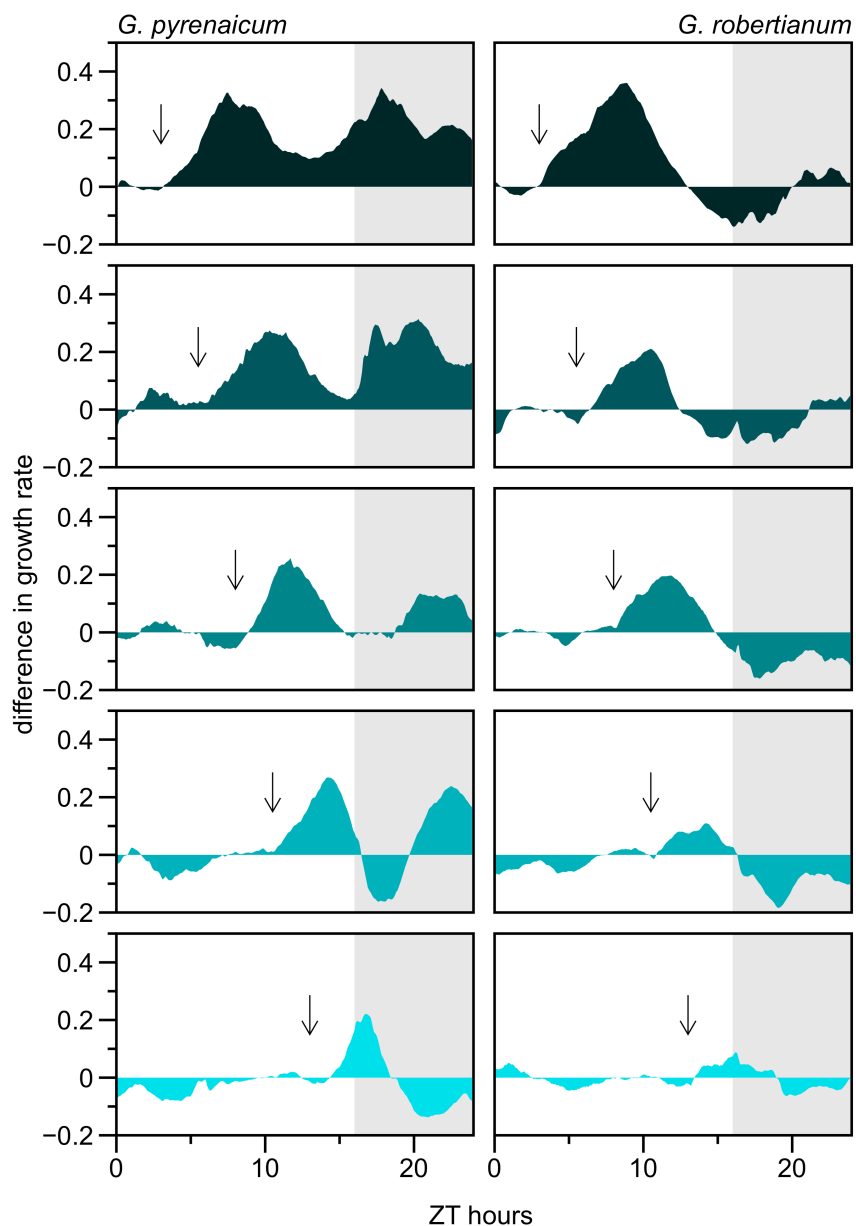
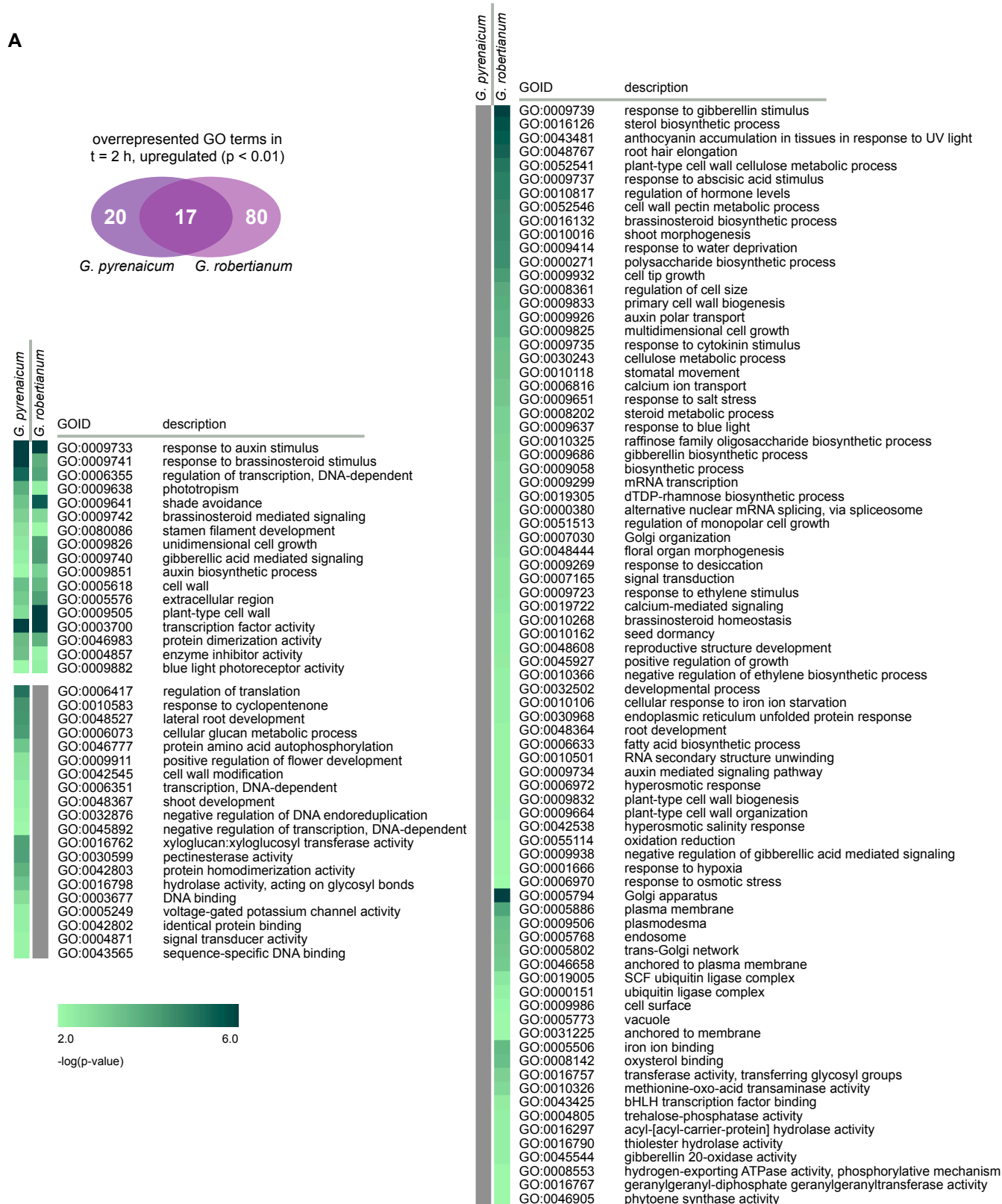


Supplemental Figure 1. A detailed analysis of low R:FR-induced growth over the time of day and in *Geranium* petioles. (Supports Figure 1.) (A) Growth rates of *G. pyrenaicum* and *G. robertianum* petioles (mm h⁻¹) over 48 h, data for every 6 minutes. Plants grown in either control white light (open circles, R:FR = 1.8) or a low R:FR treatment (dark circles R:FR = 0.2), starting at time point 0 (ZT = 3 h, indicated by an arrow). Error bars represent SEM, n = 6. The grey bars at the x-axis indicate the night periods. (B) Detailed elongation (mm 24 h⁻¹) of putative segments (1 to 8) of the *G. pyrenaicum* and *G. robertianum* petioles in control and low R:FR conditions. Data represent means ± SEM, n = 10, asterisks represent significant differences between control and low R:FR (Student's *t*-test, *p* < 0.05). (C) Representation of the 'segment' distribution over the *Geranium* petioles, of which elongation data are shown in (B).



Supplemental Figure 2. Low R:FR light suppresses petiole growth in *G. robertianum*, but not *G. pyrenaicum*, at a fixed time of the day. (Supports Figure 1.) The difference between petiole growth rates (mm h^{-1}) in control and low R:FR treatments with a different starting point during the photoperiod, in *G. pyrenaicum* (left) and *G. robertianum* (right). Starting point of the low R:FR light treatment is indicated by an arrow (top down ZT 3 h, 5.5 h, 8 h, 10.5 h and 13 h). Data are the same as presented in Figure 1D. Differences between the means of the two treatments are smoothed using exponential smoothing, $n = 6$. The grey area represents the night period.

A



Supplemental Figure 3. Gene ontology analysis on low R:FR induced and repressed *Geranium* OMCL groups. (Supports Figure 3.) Venn diagrams showing the overlap in significantly overrepresented gene ontology (GO) terms (p < 0.01) among *Geranium* OMCL groups significantly (p < 0.01) up- (A, B) or down-regulated (C, D) by the low R:FR light treatment at the first (t= 2 h, A, C) or second time point (t = 11.5 h, B, D). Heat maps present these defined GO terms with description, sorted by domain (biological process, cellular component and molecular function) and -log p-values (green for up-regulated OMCL groups, blue for down-regulated OMCL groups in low R:FR). Grey areas represent non-enriched GO terms in the specific species.

B

overrepresented GO terms in
t = 11.5 h, upregulated (p < 0.01)



G. pyrenaicum *G. robertianum*

<i>G. pyrenaicum</i>			<i>G. robertianum</i>	
GOID	description		GOID	description
GO:0052546	cell wall pectin metabolic process		GO:0009853	photorespiration
GO:0006084	acetyl-CoA metabolic process		GO:0048825	cotyledon development
GO:0016126	sterol biosynthetic process		GO:0015031	protein transport
GO:0052541	plant-type cell wall cellulose metabolic process		GO:0000059	protein import into nucleus, docking
GO:0016132	brassinosteroid biosynthetic process		GO:0010074	maintenance of meristem identity
GO:0019745	pentacyclic triterpenoid biosynthetic process		GO:0009846	pollen germination
GO:0009826	unidimensional cell growth		GO:0006457	protein folding
GO:0006633	fatty acid biosynthetic process		GO:0006275	regulation of DNA replication
GO:0009733	response to auxin stimulus		GO:0009113	purine base biosynthetic process
GO:0006816	calcium ion transport		GO:0045489	pectin biosynthetic process
GO:0009741	response to brassinosteroid stimulus		GO:0048193	Golgi vesicle transport
GO:0046658	anchored to plasma membrane		GO:0048366	leaf development
GO:0005618	cell wall		GO:0009561	megagametogenesis
GO:0009505	plant-type cell wall		GO:0032508	DNA duplex unwinding
GO:0031225	anchored to membrane		GO:0007030	Golgi organization
GO:0001510	RNA methylation		GO:0055072	iron ion homeostasis
GO:0006412	translation		GO:0000902	cell morphogenesis
GO:0009220	pyrimidine ribonucleotide biosynthetic process		GO:0000724	double-strand break repair via homologous recombination
GO:0006606	protein import into nucleus		GO:0006351	transcription, DNA-dependent
GO:0042254	ribosome biogenesis		GO:0051788	response to misfolded protein
GO:0006626	protein targeting to mitochondrion		GO:0051726	regulation of cell cycle
GO:0006406	mRNA export from nucleus		GO:0009831	plant-type cell wall modification during multidimensional cell growth
GO:0009560	embryo sac egg cell differentiation		GO:0019932	second-messenger-mediated signaling
GO:0009909	regulation of flower development		GO:0032259	methylation
GO:0009640	photomorphogenesis		GO:0006396	RNA processing
GO:0009165	nucleotide biosynthetic process		GO:0016458	gene silencing
GO:0010388	cullin deneddylation		GO:0016051	carbohydrate biosynthetic process
GO:0000741	karyogamy		GO:0009736	cytokinin mediated signaling
GO:0006164	purine nucleotide biosynthetic process		GO:0010082	regulation of root meristem growth
GO:0006094	gluconeogenesis		GO:0010107	potassium ion import
GO:0051604	protein maturation		GO:0006268	DNA unwinding during replication
GO:0034968	histone lysine methylation		GO:0006189	'de novo' IMP biosynthetic process
GO:0006261	DNA-dependent DNA replication		GO:0032875	regulation of DNA endoreduplication
GO:0006886	intracellular protein transport		GO:0030244	cellulose biosynthetic process
GO:0000398	nuclear mRNA splicing, via spliceosome		GO:0016049	cell growth
GO:0010162	seed dormancy		GO:0016579	protein deubiquitination
GO:0007010	cytoskeleton organization		GO:0010197	polar nucleus fusion
GO:0019915	lipid storage		GO:0006571	tyrosine biosynthetic process
GO:0042545	cell wall modification		GO:0006065	UDP-glucuronate biosynthetic process
GO:0009933	meristem structural organization		GO:0051510	regulation of unidimensional cell growth
GO:0006260	DNA replication		GO:0006269	DNA replication, synthesis of RNA primer
GO:0010498	proteasomal protein catabolic process		GO:0015946	methanol oxidation
GO:0009664	plant-type cell wall organization		GO:0019415	acetate biosynthetic process from carbon monoxide
GO:0006414	translational elongation		GO:0042274	ribosomal small subunit biogenesis
GO:0009845	seed germination		GO:0031538	negative regulation of anthocyanin metabolic process
GO:0006007	glucose catabolic process		GO:0031120	snRNA pseudouridine synthesis
GO:0051567	histone H3-K9 methylation		GO:0000380	alternative nuclear mRNA splicing, via spliceosome
GO:0010182	sugar mediated signaling		GO:0010501	RNA secondary structure unwinding
GO:0050826	response to freezing		GO:0016567	protein ubiquitination
GO:0009553	embryo sac development		GO:0009958	positive gravitropism
GO:0000478	endonucleolytic cleavages during rRNA processing		GO:0009793	embryonic development ending in seed dormancy
GO:0048767	root hair elongation		GO:0005840	ribosome
GO:0016192	vesicle-mediated transport		GO:0005730	nucleolus
GO:0042991	transcription factor import into nucleus		GO:0005829	cytosol
GO:0045039	protein import into mitochondrial inner membrane		GO:0022625	cytosolic large ribosomal subunit
GO:0006913	nucleocytoplasmic transport		GO:0022627	cytosolic small ribosomal subunit
GO:0006354	RNA elongation		GO:0005794	Golgi apparatus
GO:0034976	response to endoplasmic reticulum stress		GO:0022626	cytosolic ribosome
GO:0006270	DNA replication initiation		GO:0005622	intracellular
GO:0009086	methionine biosynthetic process		GO:0009506	plasmodesma
GO:0044267	cellular protein metabolic process		GO:0005802	trans-Golgi network
GO:0006334	nucleosome assembly		GO:0005774	vacuolar membrane
GO:0008283	cell proliferation		GO:0015934	large ribosomal subunit
GO:0006446	regulation of translational initiation		GO:0005768	endosome
GO:0006096	glycolysis		GO:0005737	cytoplasm
GO:0006413	translational initiation		GO:0005783	endoplasmic reticulum
GO:0006418	tRNA aminoacylation for protein translation		GO:0016020	membrane
GO:0051301	cell division		GO:0015935	small ribosomal subunit
GO:0046686	response to cadmium ion		GO:0005852	eukaryotic translation initiation factor 3 complex
GO:0044070	regulation of anion transport		GO:0005773	vacuole
			GO:0005643	nuclear pore

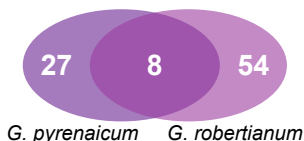
B (continued)

<i>G. pyrenaicum</i> <i>G. robertianum</i>	GOID	description	<i>G. pyrenaicum</i> <i>G. robertianum</i>	GOID	description
	GO:0005635	nuclear envelope		GO:0009641	shade avoidance
	GO:0005739	mitochondrion		GO:0009737	response to abscisic acid stimulus
	GO:0005886	plasma membrane		GO:0007623	circadian rhythm
	GO:0005743	mitochondrial inner membrane		GO:0010105	negative regulation of ethylene mediated signaling pathway
	GO:0005741	mitochondrial outer membrane		GO:0010224	response to UV-B
	GO:0000786	nucleosome		GO:0006355	regulation of transcription, DNA-dependent
	GO:0005732	small nucleolar ribonucleoprotein complex		GO:0009651	response to salt stress
	GO:0030131	clathrin adaptor complex		GO:0042538	hyperosmotic salinity response
	GO:0005758	mitochondrial intermembrane space		GO:0005975	carbohydrate metabolic process
	GO:0030173	integral to Golgi membrane		GO:0010201	response to continuous far red light stimulus by the high-irradiance response system
	GO:0030132	clathrin coat of coated pit		GO:0010218	response to far red light
	GO:0005789	endoplasmic reticulum membrane		GO:0009414	response to water deprivation
	GO:0033588	Elongator holoenzyme complex		GO:0055114	oxidation reduction
	GO:0080008	CUL4 RING ubiquitin ligase complex		GO:0080086	stamen filament development
	GO:0009986	cell surface		GO:0010017	red or far red light signaling pathway
	GO:0005753	mitochondrial proton-transporting ATP synthase complex		GO:0009739	response to gibberellin stimulus
	GO:0030117	membrane coat		GO:0009723	response to ethylene stimulus
	GO:0030126	COPI vesicle coat		GO:0048359	mucilage metabolic process during seed coat development
	GO:0015030	Cajal body		GO:0010016	shoot morphogenesis
	GO:0005759	mitochondrial matrix		GO:0009638	phototropism
	GO:0009504	cell plate		GO:0048574	long-day photoperiodism, flowering
	GO:0030130	clathrin coat of trans-Golgi network vesicle		GO:0009639	response to red or far red light
	GO:0005750	mitochondrial respiratory chain complex III		GO:0007165	signal transduction
	GO:0000790	nuclear chromatin		GO:0010325	raffinose family oligosaccharide biosynthetic process
	GO:0008250	oligosaccharyltransferase complex		GO:0043496	regulation of protein homodimerization activity
	GO:0005853	eukaryotic translation elongation factor 1 complex		GO:0010203	response to very low fluence red light stimulus
	GO:0042719	mitochondrial intermembrane space protein transporter complex		GO:0009686	gibberellin biosynthetic process
	GO:0003735	structural constituent of ribosome		GO:0009685	gibberellin metabolic process
	GO:0003723	RNA binding		GO:0048444	floral organ morphogenesis
	GO:0003743	translation initiation factor activity		GO:0009409	response to cold
	GO:0005507	copper ion binding		GO:0006073	cellular glucan metabolic process
	GO:0003676	nucleic acid binding		GO:0009740	gibberellic acid mediated signaling
	GO:0008026	ATP-dependent helicase activity		GO:0048608	reproductive structure development
	GO:0015450	P-P-bond-hydrolysis-driven protein transmembrane transporter activity		GO:0030148	sphingolipid biosynthetic process
	GO:0008565	protein transporter activity		GO:0080001	mucilage extrusion from seed coat
	GO:0003690	double-stranded DNA binding		GO:0046916	cellular transition metal ion homeostasis
	GO:0000166	nucleotide binding		GO:0000719	photoreactive repair
	GO:0005525	GTP binding		GO:0010187	negative regulation of seed germination
	GO:0008168	methyltransferase activity		GO:0030643	cellular phosphate ion homeostasis
	GO:0004812	aminoacyl-tRNA ligase activity		GO:0010366	negative regulation of ethylene biosynthetic process
	GO:0005085	guanyl-nucleotide exchange factor activity		GO:0045493	xylan catabolic process
	GO:0047262	polygalacturonate 4-alpha-galacturonosyltransferase activity		GO:0009269	response to desiccation
	GO:0051082	unfolded protein binding		GO:0006598	polyamine catabolic process
	GO:0000175	3'-5'-exoribonuclease activity		GO:0042752	regulation of circadian rhythm
	GO:0008308	voltage-gated anion channel activity		GO:0042398	cellular amino acid derivative biosynthetic process
	GO:0003697	single-stranded DNA binding		GO:0010114	response to red light
	GO:0004576	oligosaccharyl transferase activity		GO:0006071	glycerol metabolic process
	GO:0004579	dolichyl-diphosphooligosaccharide-protein glycotransferase activity		GO:0006811	ion transport
	GO:0003878	ATP citrate synthase activity		GO:0009650	UV protection
	GO:0030515	snoRNA binding		GO:0009851	auxin biosynthetic process
	GO:0008430	selenium binding		GO:0009938	negative regulation of gibberellic acid mediated signaling
	GO:0003924	GTPase activity		GO:0009813	flavonoid biosynthetic process
	GO:0003746	translation elongation factor activity		GO:0009698	phenylpropanoid metabolic process
	GO:0046914	transition metal ion binding		GO:0005576	extracellular region
	GO:0008276	protein methyltransferase activity		GO:0016604	nuclear body
	GO:0008094	DNA-dependent ATPase activity		GO:0048046	apoplast
	GO:0008143	poly(A) RNA binding		GO:0042807	central vacuole
	GO:0003979	UDP-glucose 6-dehydrogenase activity		GO:0019005	SCF ubiquitin ligase complex
	GO:0004776	succinate-CoA ligase (GDP-forming) activity		GO:0003700	transcription factor activity
	GO:0004775	succinate-CoA ligase (ADP-forming) activity		GO:0004857	enzyme inhibitor activity
	GO:0001872	zymosan binding		GO:0030599	pectinesterase activity
				GO:0004553	hydrolase activity, hydrolyzing O-glycosyl compounds
				GO:0042802	identical protein binding
				GO:0046910	pectinesterase inhibitor activity
				GO:0004190	aspartic-type endopeptidase activity
				GO:0000248	C-5 sterol desaturase activity
				GO:0005506	iron ion binding
				GO:0010326	methionine-oxo-acid transaminase activity
				GO:0042803	protein homodimerization activity
				GO:0003913	DNA photolyase activity
				GO:0008889	glycerophosphodiester phosphodiesterase activity
				GO:0000155	two-component sensor activity
				GO:0004871	signal transducer activity
				GO:0016762	xyloglucan:xyloglucosyl transferase activity
				GO:0016168	chlorophyll binding
				GO:0042284	sphingolipid delta-4 desaturase activity
				GO:0048531	beta-1,3-galactosyltransferase activity
				GO:0046608	carotenoid isomerase activity
				GO:0009882	blue light photoreceptor activity
				GO:0005249	voltage-gated potassium channel activity
				GO:0031516	far-red light photoreceptor activity
				GO:0005515	protein binding
				GO:0009044	xylan 1,4-beta-xylosidase activity



C

overrepresented GO terms in
t = 2 h, downregulated (p < 0.01)



<i>G. pyrenaicum</i>	<i>G. robertianum</i>	GOID	description
		GO:0006355	regulation of transcription, DNA-dependent
		GO:0006857	oligopeptide transport
		GO:0006612	protein targeting to membrane
		GO:0009753	response to jasmonic acid stimulus
		GO:0010075	regulation of meristem growth
		GO:0003700	transcription factor activity
		GO:0008194	UDP-glycosyltransferase activity
		GO:0016758	transferase activity, transferring hexosyl groups
		GO:0009686	gibberellin biosynthetic process
		GO:0030001	metal ion transport
		GO:0000165	MAPKKK cascade
		GO:0010310	regulation of hydrogen peroxide metabolic process
		GO:0010023	proanthocyanidin biosynthetic process
		GO:0009862	systemic acquired resistance, salicylic acid mediated signaling pathway
		GO:0009867	jasmonic acid mediated signaling pathway
		GO:0048439	flower morphogenesis
		GO:0010363	regulation of plant-type hypersensitive response
		GO:0010051	xylem and phloem pattern formation
		GO:0031348	negative regulation of defense response
		GO:0010099	regulation of photomorphogenesis
		GO:0048519	negative regulation of biological process
		GO:0009617	response to bacterium
		GO:0010161	red light signaling pathway
		GO:0009855	determination of bilateral symmetry
		GO:0010583	response to cyclopentenone
		GO:0009648	photoperiodism
		GO:0010067	procambium histogenesis
		GO:0048354	mucilage biosynthetic process during seed coat development
		GO:0009944	polarity specification of adaxial/abaxial axis
		GO:0016020	membrane
		GO:0004497	monoxygenase activity
		GO:0005506	iron ion binding
		GO:0020037	heme binding
		GO:0016705	oxidoreductase activity, acting on paired donors, with incorporation/reduction of molecular O2
		GO:0005215	transporter activity
		GO:0009963	positive regulation of flavonoid biosynthetic process
		GO:0007169	transmembrane receptor protein tyrosine kinase signaling pathway
		GO:0009741	response to brassinosteroid stimulus
		GO:0008152	metabolic process
		GO:0002237	response to molecule of bacterial origin
		GO:0009611	response to wounding
		GO:0009751	response to salicylic acid stimulus
		GO:0006468	protein amino acid phosphorylation
		GO:0006805	xenobiotic metabolic process
		GO:0009698	phenylpropanoid metabolic process
		GO:0045487	gibberellin catabolic process
		GO:0032940	secretion by cell
		GO:0009684	indoleacetic acid biosynthetic process
		GO:0009750	response to fructose stimulus
		GO:0006833	water transport
		GO:0009718	anthocyanin biosynthetic process
		GO:0009805	coumarin biosynthetic process
		GO:0006535	cysteine biosynthetic process from serine
		GO:0019953	sexual reproduction
		GO:0010167	response to nitrate
		GO:0006629	lipid metabolic process
		GO:0030003	cellular cation homeostasis
		GO:0031347	regulation of defense response
		GO:0048589	developmental growth
		GO:0000082	G1/S transition of mitotic cell cycle
		GO:0050982	detection of mechanical stimulus
		GO:0010214	seed coat development
		GO:0009809	lignin biosynthetic process
		GO:0005576	extracellular region
		GO:0070825	micropyle
		GO:0005886	plasma membrane
		GO:0016747	transferase activity, transferring acyl groups other than amino-acyl groups
		GO:0016740	transferase activity
		GO:0004713	protein tyrosine kinase activity
		GO:0008131	amine oxidase activity
		GO:0019825	oxygen binding
		GO:0016706	oxidoreductase activity
		GO:0050362	L-tryptophan:2-oxoglutarate aminotransferase activity
		GO:0080097	L-tryptophan:pyruvate aminotransferase activity
		GO:0004672	protein kinase activity
		GO:0004674	protein serine/threonine kinase activity
		GO:0051119	sugar transmembrane transporter activity
		GO:0008289	lipid binding
		GO:0016772	transferase activity, transferring phosphorus-containing groups
		GO:0016846	carbon-sulfur lyase activity
		GO:0008146	sulfotransferase activity
		GO:0080131	hydroxyjasmonate sulfotransferase activity
		GO:0017057	6-phosphogluconolactonase activity
		GO:0047172	shikimate O-hydroxycinnamoyltransferase activity
		GO:0047205	quininate O-hydroxycinnamoyltransferase activity
		GO:0016207	4-coumarate-CoA ligase activity
		GO:0008381	mechanically-gated ion channel activity
		GO:0016682	oxidoreductase activity, acting on diphenols and related substances as donors, oxygen as acceptor
		GO:0015145	monosaccharide transmembrane transporter activity



D

overrepresented GO terms in
t = 11.5 h, downregulated (p < 0.01)



G. pyrenaicum *G. robertianum*

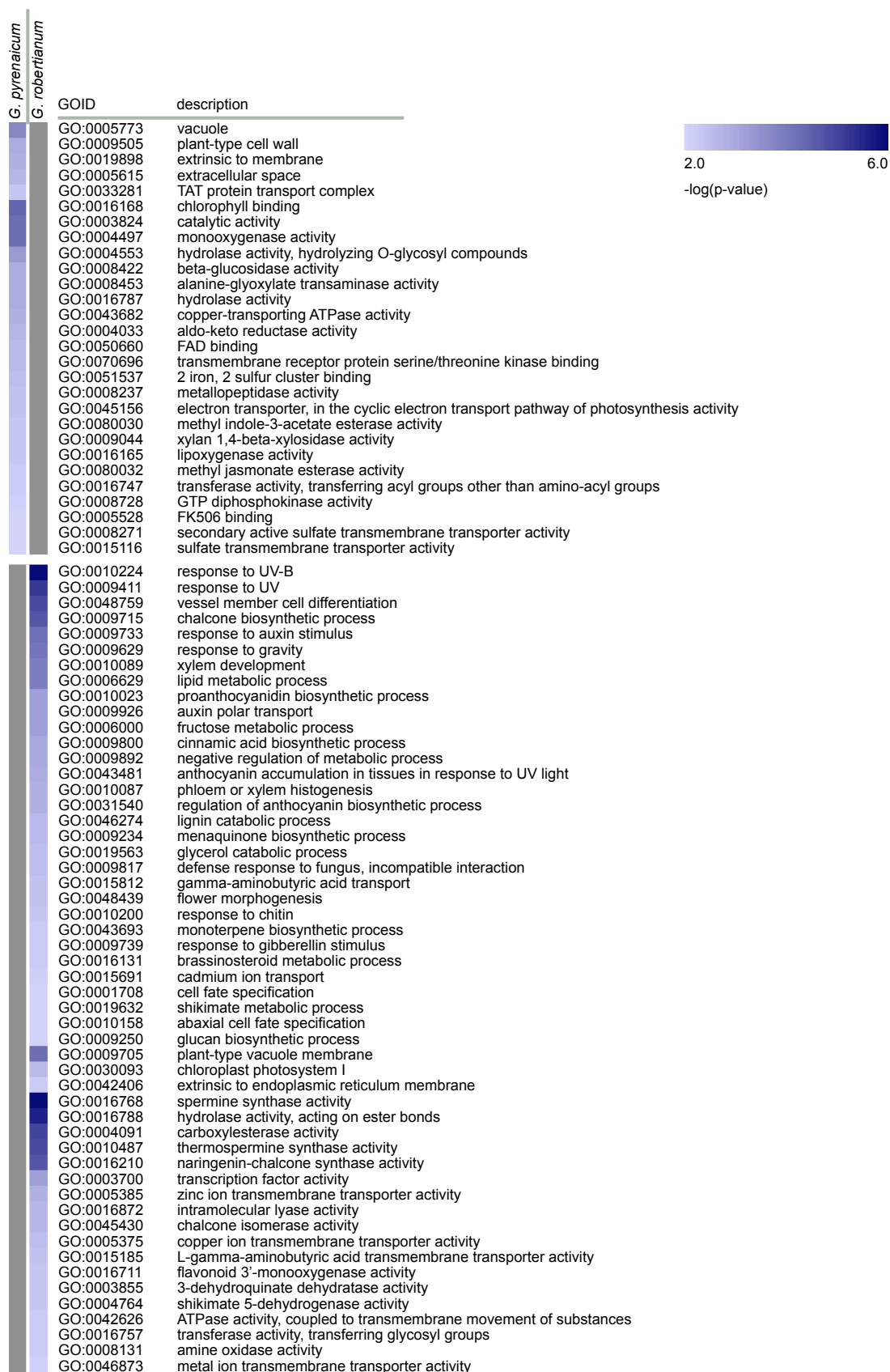
G. pyrenaicum
G. robertianum

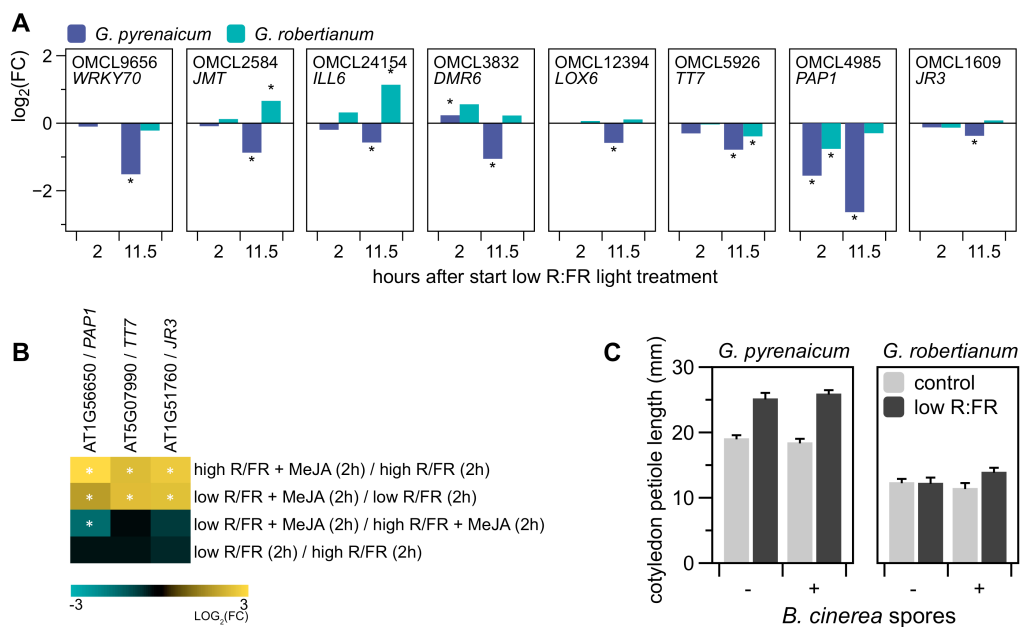
GOID	description
GO:0019684	photosynthesis, light reaction
GO:0015979	photosynthesis
GO:0006098	pentose-phosphate shunt
GO:0055114	oxidation reduction
GO:0019252	starch biosynthetic process
GO:0043085	positive regulation of catalytic activity
GO:0008152	metabolic process
GO:0010218	response to far red light
GO:0009744	response to sucrose stimulus
GO:0010310	regulation of hydrogen peroxide metabolic process
GO:0009718	anthocyanin biosynthetic process
GO:0042742	defense response to bacterium
GO:0043900	regulation of multi-organism process
GO:0009595	detection of biotic stimulus
GO:0009813	flavonoid biosynthetic process
GO:0006979	response to oxidative stress
GO:0015976	carbon utilization
GO:0010037	response to carbon dioxide
GO:0009830	cell wall modification during abscission
GO:0034484	raffinose catabolic process
GO:0009751	response to salicylic acid stimulus
GO:0009809	lignin biosynthetic process
GO:0030388	fructose 1,6-bisphosphate metabolic process
GO:0009579	thylakoid
GO:0005576	extracellular region
GO:0009570	chloroplast stroma
GO:0010319	stromule
GO:0048046	apoplast
GO:0016491	oxidoreductase activity
GO:0020037	heme binding
GO:0016705	oxidoreductase activity, acting on paired donors
GO:0009055	electron carrier activity
GO:0019825	oxygen binding
GO:0005506	iron ion binding
GO:0008194	UDP-glycosyltransferase activity
GO:0016706	oxidoreductase activity
GO:0016298	lipase activity
GO:0004185	serine-type carboxypeptidase activity
GO:0004089	carbonate dehydratase activity
GO:0015171	amino acid transmembrane transporter activity
GO:0008289	lipid binding
GO:0042132	fructose 1,6-bisphosphate 1-phosphatase activity
GO:0010207	photosystem II assembly
GO:0000023	maltose metabolic process
GO:0070838	divalent metal ion transport
GO:0009657	plastid organization
GO:0009773	photosynthetic electron transport in photosystem I
GO:0030003	cellular cation homeostasis
GO:0006364	rRNA processing
GO:0010027	thylakoid membrane organization
GO:0019761	glucosinolate biosynthetic process
GO:0009637	response to blue light
GO:0035304	regulation of protein amino acid dephosphorylation
GO:0019288	isopentenyl diphosphate biosynthetic process
GO:0010155	regulation of proton transport
GO:0016117	carotenoid biosynthetic process
GO:0015995	chlorophyll biosynthetic process
GO:0009902	chloroplast relocation
GO:0010114	response to red light
GO:0019344	cysteine biosynthetic process
GO:0010103	stomatal complex morphogenesis
GO:0016556	mRNA modification
GO:0015996	chlorophyll catabolic process
GO:0034660	ncRNA metabolic process
GO:0006612	protein targeting to membrane
GO:0010363	regulation of plant-type hypersensitive response
GO:0009611	response to wounding
GO:0009862	systemic acquired resistance, salicylic acid signaling pathway

G. pyrenaicum
G. robertianum

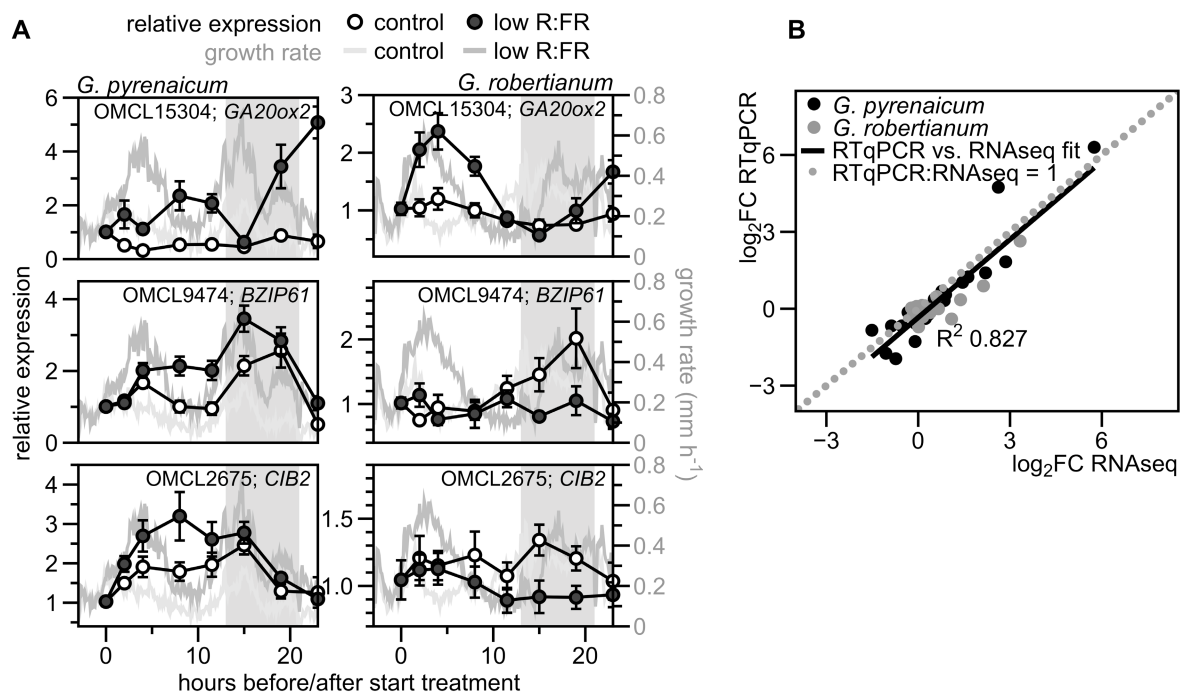
GOID	description
GO:0009765	photosynthesis, light harvesting
GO:0005975	carbohydrate metabolic process
GO:0030154	cell differentiation
GO:0010304	PSII associated light-harvesting complex II catabolic process
GO:0019760	glucosinolate metabolic process
GO:0009867	jasmonic acid mediated signaling pathway
GO:0009814	defense response, incompatible interaction
GO:0009965	leaf morphogenesis
GO:0000165	MAPKKK cascade
GO:0009409	response to cold
GO:0050832	defense response to fungus
GO:0009963	positive regulation of flavonoid biosynthetic process
GO:0006636	unsaturated fatty acid biosynthetic process
GO:0006508	proteolysis
GO:0010106	cellular response to iron ion starvation
GO:0009767	photosynthetic electron transport chain
GO:0006952	defense response
GO:0055085	transmembrane transport
GO:0009617	response to bacterium
GO:0009699	phenylpropanoid biosynthetic process
GO:0009684	indoleacetic acid biosynthetic process
GO:0010043	response to zinc ion
GO:0009750	response to fructose stimulus
GO:0042793	transcription from plastid promoter
GO:0006569	tryptophan catabolic process
GO:0009753	response to jasmonic acid stimulus
GO:0006857	oligopeptide transport
GO:0009697	salicylic acid biosynthetic process
GO:0019375	galactolipid biosynthetic process
GO:0009768	photosynthesis, light harvesting in photosystem I
GO:0015977	carbon utilization by fixation of carbon dioxide
GO:0015969	guanosine tetraphosphate metabolic process
GO:0031348	negative regulation of defense response
GO:0016036	cellular response to phosphate starvation
GO:0016120	carotene biosynthetic process
GO:0009269	response to desiccation
GO:0010264	myo-inositol hexakisphosphate biosynthetic process
GO:0042744	hydrogen peroxide catabolic process
GO:0006869	lipid transport
GO:0002238	response to molecule of fungal origin
GO:0006817	phosphate transport
GO:0009694	jasmonic acid metabolic process
GO:0046777	protein amino acid autophosphorylation
GO:0000413	protein peptidyl-prolyl isomerization
GO:0009695	jasmonic acid biosynthetic process
GO:0006655	phosphatidylglycerol biosynthetic process
GO:0010270	photosystem II oxygen evolving complex assembly
GO:0006598	polyamine catabolic process
GO:0015994	chlorophyll metabolic process
GO:0019748	secondary metabolic process
GO:0006805	xenobiotic metabolic process
GO:0010351	lithium ion transport
GO:0034440	lipid oxidation
GO:0009821	alkaloid biosynthetic process
GO:0006826	iron ion transport
GO:0019464	glycine decarboxylation via glycine cleavage system
GO:0043086	negative regulation of catalytic activity
GO:0044265	cellular macromolecule catabolic process
GO:0018208	peptidyl-proline modification
GO:0005985	sucrose metabolic process
GO:0015698	inorganic anion transport
GO:0010271	regulation of chlorophyll catabolic process
GO:0010115	regulation of abscisic acid biosynthetic process
GO:0042549	photosystem II stabilization
GO:0009698	phenylpropanoid metabolic process
GO:0009535	chloroplast thylakoid membrane
GO:0009507	chloroplast
GO:0009534	chloroplast thylakoid
GO:0009941	chloroplast envelope
GO:0010287	plastoglobule
GO:0031977	thylakoid lumen
GO:0009543	chloroplast thylakoid lumen
GO:0030095	chloroplast photosystem II
GO:0009522	photosystem I
GO:0009523	photosystem II
GO:0009654	oxygen evolving complex
GO:0010598	NAD(P)H dehydrogenase complex (plastoquinone)
GO:0030076	light-harvesting complex
GO:0005777	peroxisome
GO:0009538	photosystem I reaction center
GO:0016020	membrane

D (continued)

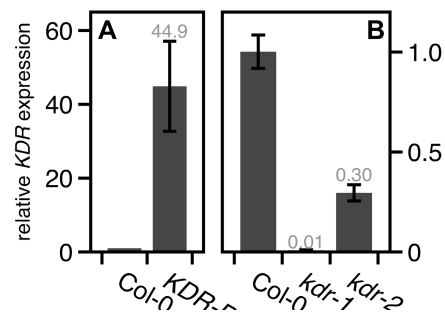




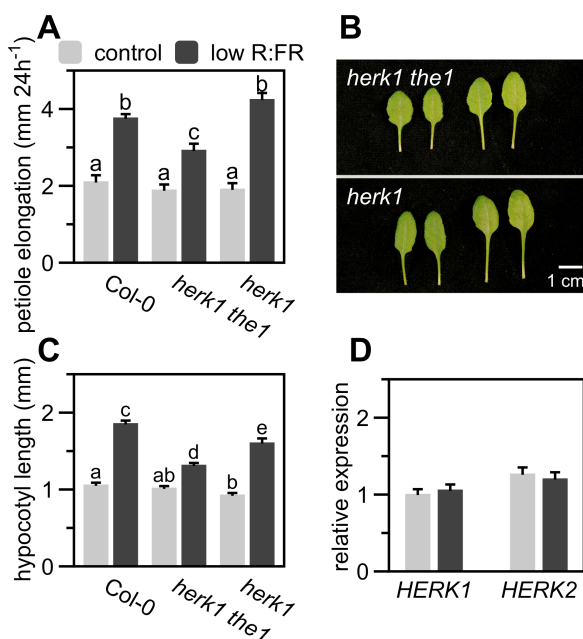
Supplemental Figure 5. Low R:FR light affects meJA-induced transcript abundance in the Geraniums and *A. thaliana*, and pathogen infection does not affect *Geranium* growth in the shade. (Supports Figure 4.) (A) Log_2 fold-changes of a subset of OMCL groups from the GO clusters shown in Fig. 4A. Asterisks represent significant differences between low R:FR and control ($p < 0.01$, qCML method, followed by an exact test). (B) Heat map representing log fold changes for *PAP1*, *TT7* and *JR3*, upon a meJA (100 μM) treatment in a control (R:FR = 1.8) or low (R:FR = 0.2) R:FR light environment in *A. thaliana*. Samples harvested 2 hours after start of the hormone and light treatment, $n = 3$. Asterisks represent a significant difference between the presented conditions ($p < 0.01$). Data taken from de Wit et al., 2013. (C) Petiole length of *G. pyrenaicum* (left) and *G. robertianum* (right) cotyledons (mm), with or without *B. cinerea* infection, in a control (R:FR = 1.8) or low R:FR (R:FR = 0.2) light treatment. Data represent means + SEM, $n = 28$.



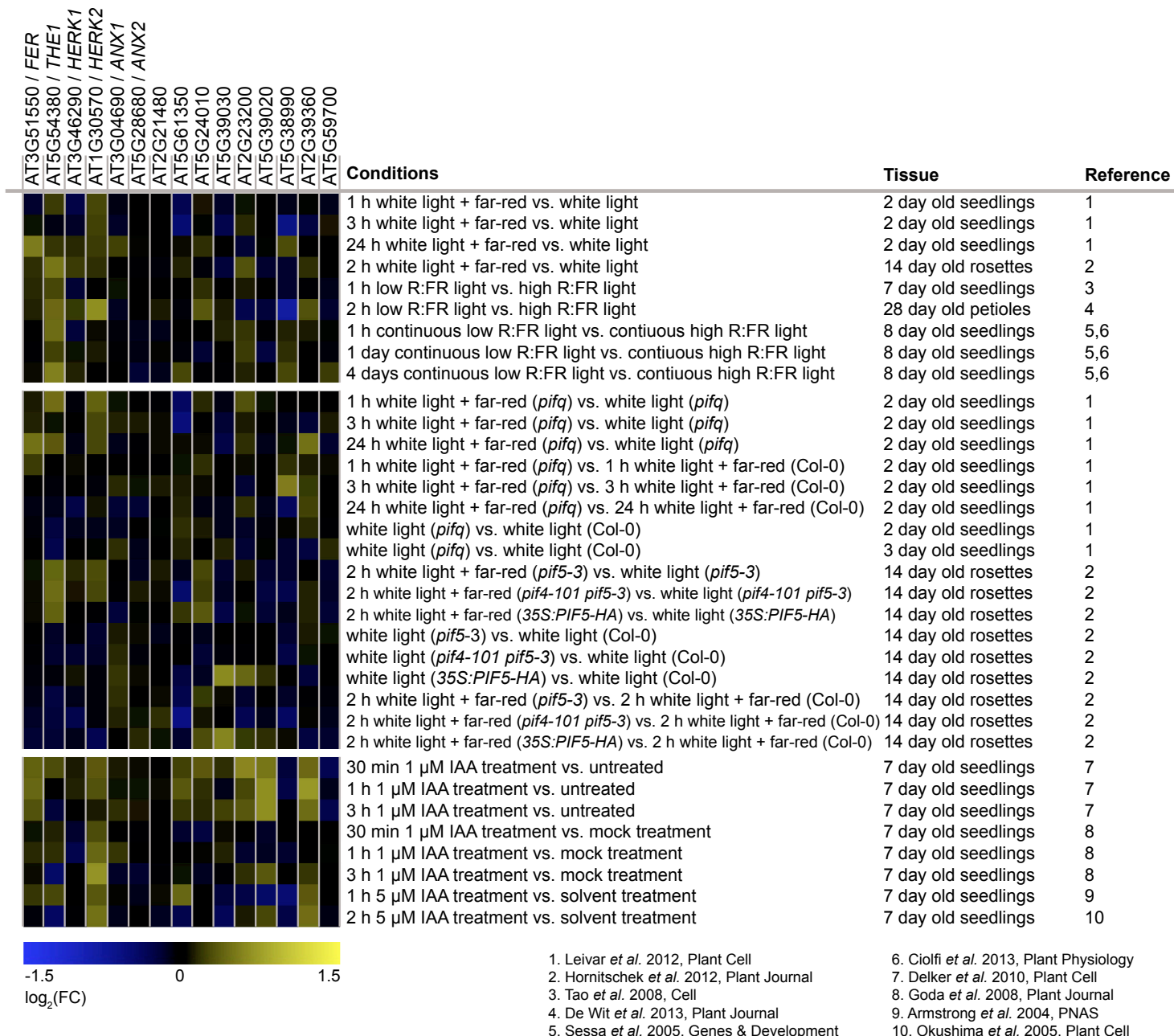
Supplemental Figure 6. RT qPCR on *Geranium* transcripts and validation of RNA sequencing. (Supports Figure 6.) (A) Relative OMCL group expression (orthologues of *GA20OX2*, *BZIP61* and *CIB2*) over time in *G. pyrenaicum* (left panels) and *G. robertianum* (right panels) in control (R:FR = 1.8; open circles) and low R:FR (R:FR = 0.2; dark circles) conditions, on the left y-axis. Data are relative to the reference gene (orthologue of *PDF1*) and to $t = 0$ (10:00 am), data represent means \pm SEM, $n = 5$ (biological replicates are a pool of the second petiole of three individual plants). Right y-axis and grey lines represent growth rates in mm h^{-1} over the same time period in control (light grey) and low R:FR (darker grey) conditions (same data as Fig. 1C). Grey area represents the night period. (B) Comparison of the \log_2 fold-changes of several OMCL groups determined by RNAseq (x-axis) and real-time quantitative PCR (y-axis). Analyses were performed on a different set of samples, harvested under the same conditions; low R:FR vs. control light, $t = 2$ h and $t = 11.5$ h.



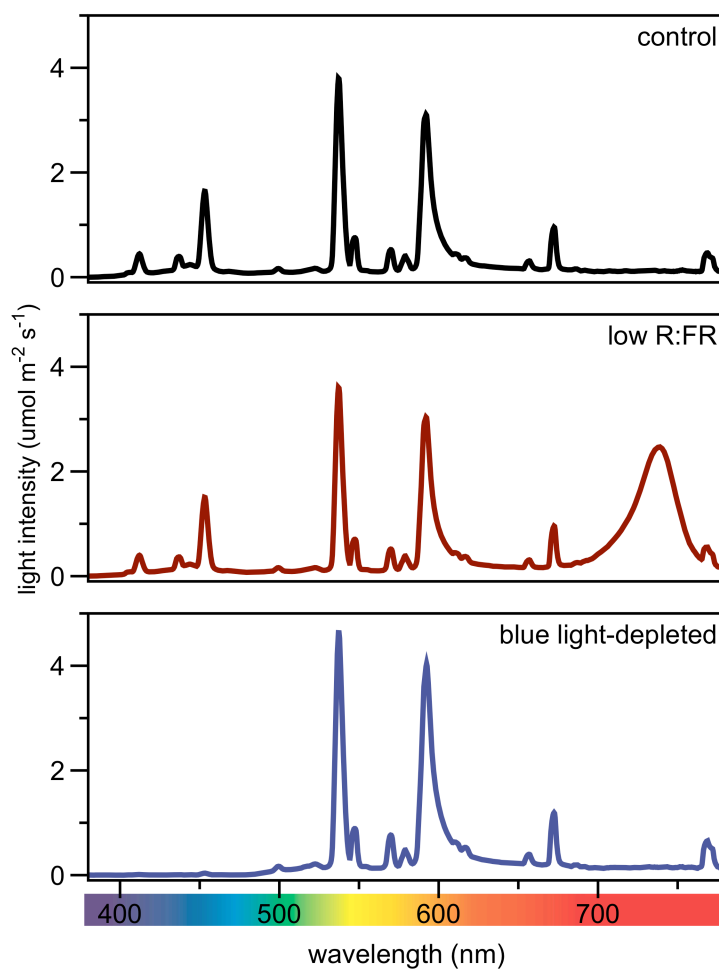
Supplemental Figure 7. Confirmation of *kdr* mutants. (Supports Figure 7.) (A and B) Relative *KDR* expression in Col-0 wild-type, *KDR* over-expressing *KDR-D* (A) and knock-out *kdr-1* and knock-down *kdr-2* (B), relative to Col-0 and reference genes *UBQ5* (*KDR-D*) and *APT* (*kdr-1* and *kdr-2*). Data represent means \pm SEM, n = 2-3.



Supplemental Figure 8. HERK1 has no function in the *A. thaliana* shade avoidance syndrome. (Supports Figure 7.) (A) Petiole elongation (mm 24 h⁻¹) of *A. thaliana* *herk1the1* and *herk1* mutants, and WT control (Col-0), grown in control white light (R:FR = 1.8) or low R:FR (R:FR = 0.2) conditions. Data represent means + SEM, n = 10. Different letters indicate significant differences (p < 0.05, 2-way ANOVA with post-hoc Tukey test). (B) Pictures of representative leaves of *herk1the1* and *herk1* grown for five days in control white light (left pair) or low R:FR (right pair) conditions. (C) Hypocotyl length (mm) of lines shown in (A), after four days of control white light or low R:FR treatment. Data represent means + SEM, n = 40. Different letters indicate significant differences (p < 0.05, 2-way ANOVA with post-hoc Tukey test). (D) Relative expression of *HERK1* and *HERK2* in *A. thaliana* (Col-0) petioles exposed to control white or low R:FR light for 4 hours. Data represent means + SEM, data is relative to reference genes and control, n = 6.



Supplemental Figure 9. RLK gene expression is hardly affected by low R:FR, *pif* mutations and IAA in previous transcriptome studies. (Supports Figure 9.) Heatmap showing transcriptional Log₂ fold-changes of *THE1*, *FER* and several other RLK-encoding genes in previous micro-array studies with various R:FR ratios, different *pif*-deficient and over-expressing mutants, and IAA treatments. Data were obtained via the Genevestigator programme and numbers refer to the publications of the original datasets.



Supplemental Figure 10. Light spectra of the treatments used in this study. Light spectra of control white light (R:FR = 1.8, upper), low R:FR (0.2, middle) and blue light-depleted (R:FR = 1.8, 4 μmol m⁻² s⁻¹ B, lower) treatments, given in μmol m⁻² s⁻¹ nm⁻¹.

Supplemental Table 1. List of all primers used for RT qPCR on *G. pyrenaicum*, *G. robertianum* and *A. thaliana* in this study.

Species	OMCL group	Description	Forward	Reverse
<i>G. pyrenaicum</i>	OMCL1609	<i>JR3</i>	TTTTGCCCTTCACCTCGTT	ATGCCACACTACCATGCTC
	OMCL5926	<i>TT7</i>	ATCTTCCTGAACAAGCGCCA	GAGCCAAACACGTCGCTTAC
	OMCL4985	<i>PAP1</i>	TCAACCACCTCAGTCTACAGC	TGGTGAAGGAAGATGGCACC
	OMCL14968	<i>KDR</i>	CATGATCTCCGACGACCAGA	CTTGCAACACCTTCGAAGCT
	OMCL1872	<i>THE1</i>	GGGCCACACAGCAACAATAA	TTCTTCTTCGTCGGCAGAT
	OMCL2164	<i>FER</i>	CAGCAGGGTACGTAACAGTC	ACGGGATTGTTTCAGGTCATG
	OMCL15305	<i>GA20OX2</i>	ATTACCACGCACACTCCCTT	CGGGCCTGATTTTGAACCAA
	OMCL2675	<i>CIB</i>	TTCCAAGGTTGCATCAGAGG	GCTCCAAATTGCCGTCTTTC
	OMCL9475	<i>BZIP61</i>	AGTGGTGCGTTCTGGCTAAA	TGTCACAATCTGGCCCCATC
OMCL703	<i>PDF1 (ref.)</i>	TCTGGAGACCTTTGCTCTG	CCACCAGATCACTCTCCCTC	
<i>G. robertianum</i>	OMCL1609	<i>JR3</i>	CCCRACTGTGAACGATCCAA	CGGTGAAAGTTGGAGCCAGT
	OMCL5926	<i>TT7</i>	TCTCGCCCAACAACAGAGTC	GACGTCAAGCACTGTGGAGT
	OMCL4985	<i>PAP1</i>	TCGCTGTTCTTCCAAACCCA	TGATCCAGCTTTTCGACCACA
	OMCL14968	<i>KDR</i>	GGATGATTTGAGCGAGCGTT	TGCGAATAATGGCTGCTTGA
	OMCL1872	<i>THE1</i>	AGGTTGAAGTTTCCGTTGCC	ACACCCGAAACAGCTCCTAA
	OMCL2164	<i>FER</i>	GTCATGTTCCGATCAGCAGT	CGGGACTGTTTAGGTCATGG
	OMCL15305	<i>GA20OX2</i>	CTGCCACTTGTTTTCCGGTGA	TCAGGATTGACACTCGGGAC
	OMCL2675	<i>CIB</i>	TGCTCAACCTTCATATGCC	TCGGGATTCTGAGACGATGA
	OMCL9475	<i>BZIP61</i>	TTACCGCCCAAAGTACCGAC	AGTCGTCCACCCAACAAGTT
OMCL703	<i>PDF1 (ref.)</i>	CCAGAGGCGATGAAGACTGA	TTCCCAAGTTTGATGCAGC	
<i>A. thaliana</i>		<i>KDR</i>	CAACACCTCATCCCTGAACT	ACGGTCACTGAGGTCATCAAC
		<i>THE1</i>	GTTCTTTGGTTGGTGCGGTT	TTCTTGAGGACTCGTCGACC
		<i>FER</i>	GGTTTCTTCCCGATTCTTCAG	AGAAGAAGAAGAGAGACGGAA
		<i>IAA19</i>	GCTGTAAGGAAGCTTCGACC	ACCATCTTTCAAGGCCACAC
		<i>ATHB2</i>	CGAGCAAGACAAGTGAAGT	ATTCTCGCAGCATCTCCGTA
		<i>HERK1</i>	TCCTTTCATGGGACCGTTACT	CCATGGCAGATACAAAGCAAGA
		<i>HERK2</i>	TCGACTGGTCACTCGGTAAG	TGCTTCGCCTTTTCTTGCAT
		<i>APT1 (ref.)</i>	AATGGCGACTGAAGATGTGC	TCAGTGTGAGAAGAAGCGT
		<i>AT1G13320 (ref.)</i>	GTAGGACCGGAGCCAAGTAG	ACAGGGAAGAATGTGCTGGA
		<i>UBQ5 (ref.)</i>	CGGACCAGCAGCGATTGATT	CCTCTTCTTAGCACCACCAG
		<i>AT4G26410 (ref.)</i>	ATTGGTGTGCTGCTAGTCT	TAAAGCCGTCTCTCAAGCA